WIDEBAND FRACTIONAL DELAY FILTER DESIGN BASED ON INTERLACED SAMPLING METHOD

Chien-Cheng Tseng[1] *and Su-Ling Lee*[2]

[1]Depart. of Computer and Communication Engineering
National Kaohsiung First University of Sci. and Tech.
Kaohsiung, Taiwan
tcc@ccms.nkfust.edu.tw

[2]Depart. of Computer Sci. and Information Engi.
Chung-Jung Christian University
Tainan, Taiwan
lilee@mail.cjcu.edu.tw

ABSTRACT

In this paper, the design of wideband fractional delay filter is investigated. First, the reconstruction formula of interlaced sampling method is applied to design wideband fractional delay filter by using index substitution and window method. The filter coefficients are easily computed because closed-form design is obtained. Then, the weighted least squares method is used to design wideband fractional delay filters. Finally, numerical examples are demonstrated to show that the proposed method has smaller design error than the conventional fractional delay filter without using the interlaced sampling scheme.

1. INTRODUCTION

In many signal processing applications, there is a need for a delay that is a fraction of the sampling period. These applications include beam steering of antenna array, time adjustment in digital receivers, modeling of music instruments, speech coding and synthesis, image interpolation and comb filter design etc [1]-[8]. An excellent survey of the fractional delay filter design is presented in tutorial paper [1]. The ideal frequency response of fractional delay filter is given by

$$H_d(\omega) = e^{-j\omega D} \tag{1}$$

where D is a positive real number in the desired range. So far, the fractional delay filters are all designed under the Shannon sampling scheme, as shown in Fig.1. Usually, the Shannon sampling scheme is implemented by using one analog-to-digital (ADC) converter. In this case, the frequency response of the FIR filter used to approximate this specification is given by

$$H(e^{j\omega}) = \sum_{k=0}^{N} h(k) e^{-j\omega k} \tag{2}$$

Thus, the traditional design problem is how to determine the filter $H(z)$ such that the actual frequency response $H(e^{j\omega})$ fits the ideal response $H_d(\omega)$ as well as possible. Until now, several methods have been proposed to solve this design problem such as window method, Lagrange interpolation method, maximally flat method, weighted least squares method and discrete Fourier transform method etc. In these designs, the frequency response error is defined by

$$E_1(\omega) = H(e^{j\omega}) - H_d(\omega) \tag{3}$$

If the filter coefficients $h(k)$ in Eq.(2) are real-valued, the frequency response error at $\omega = \pi$ is given by

$$\begin{aligned} E_1(\pi) &= H(e^{j\pi}) - H_d(\pi) \\ &= H(-1) - e^{-j\pi D} \\ &= [H(-1) - \cos(\pi D)] + j\sin(\pi D) \end{aligned} \tag{4}$$

Thus, the absolute value of error $E_1(\pi)$ can be written as

$$\begin{aligned} |E_1(\pi)| &= \sqrt{[H(-1) - \cos(\pi D)]^2 + [\sin(\pi D)]^2} \\ &\geq |\sin(\pi D)| \end{aligned} \tag{5}$$

So, there is an irreducible error at $\omega = \pi$ for conventional designs [2]. This means that the wideband fractional delay filter design can not be achieved by using Shannon sampling scheme in Fig.1. Therefore, it is interesting to use other sampling methods to design wideband fractional delay filter.

In the literature, there exist various sampling methods except the Shannon sampling scheme. Some typical ones are band-pass sampling, interlaced sampling, derivative sampling and generalized sampling etc [9][10]. Thus, it is interesting to design wideband fractional delay filter based on these sampling schemes. In this paper, we will use the interlaced sampling method to design fractional delay filter which is composed of two filters $G_1(z)$ and $G_2(z)$, as depicted in Fig.2. Usually, the interlaced sampling scheme is implemented by using two parallel analog-to-digital converters with different control clocks. Because $x(n-\tau)$ is the delayed version of $x(n)$, it is easy to show that the frequency-domain relation between input and output in Fig.2 is given by

$$\frac{Y(e^{j\omega})}{X(e^{j\omega})} = G_1(e^{j\omega}) + e^{-j\omega\tau} G_2(e^{j\omega}) \tag{6}$$

where $X(e^{j\omega})$ and $Y(e^{j\omega})$ are the Fourier transforms of $x(n)$ and $y(n)$. Thus, the design problem is how to determine the filters $G_1(z)$ and $G_2(z)$ such that the actual frequency response $G_1(e^{j\omega}) + e^{-j\omega\tau} G_2(e^{j\omega})$ approximates the ideal response $H_d(\omega)$ as well as possible. In this case, the frequency response error is defined by

$$E_2(\omega) = G_1(e^{j\omega}) + e^{-j\omega\tau} G_2(e^{j\omega}) - H_d(\omega) \tag{7}$$

So, the error at $\omega = \pi$ for real valued filters $G_1(z)$ and $G_2(z)$ is given by

$$\begin{aligned} &E_2(\pi) \\ &= G_1(e^{j\pi}) + e^{-j\pi\tau} G_2(e^{j\pi}) - H_d(\pi) \\ &= G_1(-1) + [\cos(\pi\tau) - j\sin(\pi\tau)]G_2(-1) - e^{-j\pi D} \\ &= [G_1(-1) + \cos(\pi\tau)G_2(-1) - \cos(\pi D)] \\ &\quad - j[\sin(\pi\tau)G_2(-1) + \sin(\pi D)] \end{aligned} \tag{8}$$

Thus, the absolute value of the error $E_2(\pi)$ can be written as

$$|E_2(\pi)| = \sqrt{\begin{aligned}&[G_1(-1) + \cos(\pi\tau)G_2(-1) - \cos(\pi D)]^2 \\ &+ [\sin(\pi\tau)G_2(-1) + \sin(\pi D)]^2\end{aligned}} \tag{9}$$

If the filters $G_1(z)$ and $G_2(z)$ are designed to satisfy the following two equalities:

$$G_1(-1) + \cos(\pi\tau)G_2(-1) = \cos(\pi D) \tag{10a}$$

$$\sin(\pi\tau)G_2(-1) = -\sin(\pi D) \tag{10b}$$

then the error $E_2(\pi)$ will reduce to zero. This means that the wideband fractional delay filter design can be achieved by using interlaced sampling scheme. The design details will be studied in next sections.

2. WINDOW METHOD

In this section, the interlaced sampling method is first reviewed. Then, we apply this method to design fractional delay filter by using window approach. Finally, numerical example is used to compare the proposed approach with conventional window method based on Shannon sampling scheme.

2.1 Design Method

Let $x(n)$ and $x(n-\tau)$ be the uniform samples of the band-limited signal $x(t)$ and its delayed signal $x(t-\tau)$, then the $x(t)$ can be reconstructed by using the formula:

$$x(t) = \sum_{m=-\infty}^{\infty} x(m)a(t-m) + \sum_{m=-\infty}^{\infty} x(m-\tau)b(t-m+\tau) \tag{11}$$

where

$$a(t) = sinc(2t) + \pi\cot(\tau\pi)\cdot t\cdot sinc^2(t) \tag{12}$$

$$b(t) = sinc(2t) - \pi\cot(\tau\pi)\cdot t\cdot sinc^2(t) \tag{13}$$

with $sinc(t) = \sin(\pi t)/\pi t$. The proof of this formula can be found in [9][10]. In the following, the index substitution and window method will be used to obtain two filters $G_1(z)$ and $G_2(z)$ in Fig.2. Using the index substitution $m = n - k$, Eq.(11) can be rewritten as

$$\begin{aligned} x(t) = &\sum_{k=-\infty}^{\infty} x(n-k)a(t-n+k) \\ &+ \sum_{k=-\infty}^{\infty} x(n-\tau-k)b(t-n+k+\tau) \end{aligned} \tag{14}$$

Taking $t = n - D$, then Eq.(14) can be expressed as

$$\begin{aligned} x(n-D) = &\sum_{k=-\infty}^{\infty} x(n-k)a(k-D) \\ &+ \sum_{k=-\infty}^{\infty} x(n-\tau-k)b(k+\tau-D) \end{aligned} \tag{15}$$

Define $\hat{g}_1(k)$ and $\hat{g}_2(k)$ as

$$\hat{g}_1(k) = a(k-D) \tag{16a}$$

$$\hat{g}_2(k) = b(k+\tau-D) \tag{16b}$$

then Eq.(15) can be rewritten as

$$\begin{aligned} &x(n-D) \\ &= \sum_{k=-\infty}^{\infty} \hat{g}_1(k)x(n-k) + \sum_{k=-\infty}^{\infty} \hat{g}_2(k)x(n-\tau-k) \\ &= \hat{g}_1(n) * x(n) + \hat{g}_2(n) * x(n-\tau) \end{aligned} \tag{17}$$

where notation $*$ denotes the operator of convolution sum. Taking the discrete-time Fourier transform at both sides of Eq.(17), we get

$$e^{-j\omega D} X(e^{j\omega}) = \begin{pmatrix} \sum_{k=-\infty}^{\infty} \hat{g}_1(k)e^{-j\omega k} + \\ e^{-j\omega\tau} \sum_{k=-\infty}^{\infty} \hat{g}_2(k)e^{-j\omega k} \end{pmatrix} X(e^{j\omega}) \tag{18}$$

where $e^{-j\omega\tau}X(e^{j\omega})$ is the Fourier transform of $x(n-\tau)$. Canceling the $X(e^{j\omega})$ at both sides of Eq.(18), we have

$$e^{-j\omega D} = \sum_{k=-\infty}^{\infty} \hat{g}_1(k)e^{-j\omega k} + \left(\sum_{k=-\infty}^{\infty} \hat{g}_2(k)e^{-j\omega k}\right)e^{-j\omega\tau} \tag{19}$$

Based on the above results, we choose two filters $G_1(z)$ and $G_2(z)$ in Fig.1(b) as

$$G_1(z) = \sum_{k=N_{1b}}^{N_{1u}} g_1(k)z^{-k} \tag{20a}$$

$$G_2(z) = \sum_{k=N_{2b}}^{N_{2u}} g_2(k)z^{-k} \tag{20b}$$

where filter coefficients $g_1(k)$ and $g_2(k)$ are obtained from $\hat{g}_1(k)$ and $\hat{g}_2(k)$ by using window approach below:

$$g_i(k) = w_i(k)\hat{g}_i(k) \qquad i = 1,2 \tag{21}$$

with

$$w_i(k) = \begin{cases} 1 & N_{ib} \le k \le N_{iu} \\ 0 & otherwise \end{cases} \tag{22}$$

The length of window $w_i(k)$ is $N_{iu} - N_{ib} + 1$. From Eq.(16), we know that the center of window interval $[N_{ib}, N_{iu}]$ should be close to the delay D for reducing the truncation error caused by windowing. So far, the interlaced sampling design has been described. Now, let us study the implementation complexity. From Fig.1 and Fig.2, it is clear that the implementation complexity can be divided into ADC part and filter part. In the filter part, the complexity of the proposed filters $G_1(z)$, $G_2(z)$ and conventional filter $H(z)$ can be evaluated by using Eq.(2) and Eq.(20). If the direct-form realization is used, the number of adders and multipliers to implement filter $H(z)$ in Fig.1 are N and $N+1$, while the number of adders and multipliers to implement FIR filters $G_1(z)$ and $G_2(z)$ in Fig.2 are $\sum_{i=1}^{2}(N_{iu}-N_{ib})$ and $\sum_{i=1}^{2}(N_{iu}-N_{ib}+1)$. In the ADC part, it can be observed that the interlaced sampling method needs one more ADC than the Shannon sampling method. In the next subsection, one numerical example will be studied.

2.2 Design Example and Comparison

In the following, one numerical example performed with MATLAB language in an IBM PC compatible computer is used to demonstrate the effectiveness of the proposed window method. To evaluate the performance, the normalized root mean squares (NRMS) error is defined by

$$E = \left(\frac{\int_0^{\pi} \left| G(e^{j\omega}) - H_d(\omega) \right|^2 d\omega}{\int_0^{\pi} \left| H_d(\omega) \right|^2 d\omega} \right)^{\frac{1}{2}} \times 100\,\% \tag{23}$$

where $G(e^{j\omega}) = G_1(e^{j\omega}) + e^{-j\omega\tau} G_2(e^{j\omega})$ in the proposed design approach. Obviously, the smaller NRMS error E is, the better performance the design method is. If $G(e^{j\omega})$ in Eq.(23) is changed to $H(e^{j\omega})$, E is the NRMS error of conventional design. In this paper, the E is computed by using numerical rectangular integration method with step size $\frac{\pi}{1000}$. Now, let us study an example below:

Example 1: In this example, we will compare the proposed method with conventional window method based on Shannon sampling scheme. To achieve this purpose, the conventional window method is briefly described below: Taking the inverse discrete-time Fourier transform of ideal frequency response $H_d(\omega)$, the ideal impulse response is given by

$$\begin{aligned} h_{id}(k) &= \frac{1}{2\pi} \int_{-\pi}^{\pi} H_d(\omega) e^{j\omega k} d\omega \\ &= sinc\ (k-D) \end{aligned} \tag{24}$$

In the conventional window method, the filter coefficients $h(k)$ in Eq.(2) are given by

$$h(k) = w(k) h_{id}(k) \tag{25}$$

where $w(k)$ is a prescribed window function of length $N+1$. A numerical example is now studied. The parameters are chosen as $N_{1b} = N_{2b} = 41$, $N_{1u} = N_{2u} = 60$, $\tau = 0.5$ and $N = 100$. Fig.3 shows the NRMS error curve E (solid line) of the proposed method for various delay D with step size $\frac{1}{40}$. The dashed line is the result of conventional rectangular window method based on Shannon sampling scheme with $w(k)=1$ for $0 \le k \le N$. It is clear that the error of proposed method is smaller than the conventional method. Fig.4(a)(b) show the magnitude response and group delay of fractional delay filter designed by proposed method for $\tau = 0.5$, $N_{1b} = N_{2b} = 41$, $N_{1u} = N_{2u} = 60$ and $D = 50.4$. Fig.4(c)(d) show the magnitude response and group delay of fractional delay filter designed by conventional rectangular window method for $N = 100$ and $D = 50.4$. Obviously, the proposed method has smaller design error in the high frequency range than Shannon sampling method. That is, the wideband design can be accomplished by the proposed method based on interlaced sampling scheme. Now, the complexity issue is addressed. Because $N_{1b} = N_{2b} = 41$, $N_{1u} = N_{2u} = 60$ and $N = 100$ are chosen, the number of adders and multipliers to implement two filters $G_1(z)$ and $G_2(z)$ are 38 and 40, while the number of adders and multipliers to implement filter $H(z)$ are 100 and 101. Obviously, the implementation complexity of $G_1(z)$ and $G_2(z)$ is smaller than that of $H(z)$. Although the filter-part accuracy and complexity of proposed method is better than conventional method, the proposed method needs one more ADC than the conventional method, as shown in Fig.1 and Fig.2. Thus, the improvement in filter part is at the cost of the increase of complexity in the ADC part.

3. WEIGHTED LEAST SQUARES METHOD

In this section, the weighted least squares (WLS) method is first used to design fractional delay filter whose coefficients can be obtained by solving matrix inversion. Then, numerical comparison with conventional WLS design is made.

3.1 Design method

Taking $z = e^{j\omega}$, the frequency response of filters $G_1(z)$ and $G_2(z)$ in Eq.(20) can be written as

$$G_i(e^{j\omega}) = \sum_{k=N_{ib}}^{N_{iu}} g_i(k) e^{-j\omega k} \qquad i = 1,2 \tag{26}$$

Thus, the frequency response $G_1(e^{j\omega}) + e^{-j\omega\tau} G_2(e^{j\omega})$ is gotten as

$$\begin{aligned} &G(e^{j\omega}) \\ &= G_1(e^{j\omega}) + e^{-j\omega\tau} G_2(e^{j\omega}) \\ &= \sum_{k=N_{1b}}^{N_{1u}} g_1(k) e^{-j\omega k} + \sum_{k=N_{2b}}^{N_{2u}} g_2(k) e^{-j\omega(k+\tau)} \end{aligned} \tag{27}$$

Defining the following four vectors

$$\boldsymbol{g}_1 = [g_1(N_{1b}) \quad g_1(N_{1b}+1) \quad \cdots \quad g_1(N_{1u})]^T \tag{28a}$$

$$\boldsymbol{g}_2 = [g_2(N_{2b}) \quad g_2(N_{2b}+1) \quad \cdots \quad g_2(N_{2u})]^T \tag{28b}$$

$$\boldsymbol{e}_1(\omega) = [e^{-j\omega N_{1b}} \quad e^{-j\omega(N_{1b}+1)} \quad \cdots \quad e^{-j\omega N_{1u}}]^T \tag{28c}$$

$$\boldsymbol{e}_2(\omega) = [e^{-j\omega(N_{2b}+\tau)} \quad e^{-j\omega(N_{2b}+1+\tau)} \quad \cdots \quad e^{-j\omega(N_{2u}+\tau)}]^T \tag{28d}$$

then the frequency response in Eq.(27) can be rewritten as

$$G(e^{j\omega}) = \boldsymbol{g}_1^T \boldsymbol{e}_1(\omega) + \boldsymbol{g}_2^T \boldsymbol{e}_2(\omega) \\ = \boldsymbol{g}^T \boldsymbol{e}(\omega) \tag{29}$$

where two vectors are

$$\boldsymbol{g} = [\boldsymbol{g}_1^T \quad \boldsymbol{g}_2^T]^T \tag{30a}$$

$$\boldsymbol{e}(\omega) = [\boldsymbol{e}_1(\omega)^T \quad \boldsymbol{e}_2(\omega)^T]^T \tag{30b}$$

For WLS design, the filter coefficient vector $\boldsymbol{g}$ is determined by minimizing the following error function:

$$J_1(\boldsymbol{g}) = \int_{-\pi}^{\pi} W(\omega)\,|\,G(e^{j\omega}) - H_d(\omega)\,|^2\ d\omega \tag{31}$$

where $W(\omega)$ is a nonnegative weighting function. Substituting Eq.(29) into Eq.(31) and using the conjugate symmetry $H_d(-\omega) = H_d(\omega)^*$, we get

$$J_1(\boldsymbol{g}) = \int_{-\pi}^{\pi} W(\omega)\,|\,\boldsymbol{g}^T\boldsymbol{e}(\omega) - H_d(\omega)\,|^2\ d\omega \\ = \boldsymbol{g}^T\boldsymbol{Q}\boldsymbol{g} - 2\boldsymbol{g}^T\boldsymbol{q} + c \tag{32}$$

where matrix $\boldsymbol{Q}$, vector $\boldsymbol{q}$, and scalar c are given by

$$\boldsymbol{Q} = 2\int_0^{\pi} W(\omega)\,\mathrm{Re}[\,\boldsymbol{e}(\omega)\boldsymbol{e}(\omega)^H\,]d\omega \tag{33a}$$

$$\boldsymbol{q} = 2\int_0^{\pi} W(\omega)\,\mathrm{Re}[\,\boldsymbol{e}(\omega)^* H_d(\omega)]d\omega \tag{33b}$$

$$c = 2\int_0^{\pi} W(\omega)\,|\,H_d(\omega)\,|^2\ d\omega \tag{33c}$$

The above superscript H denotes the Hermitian and $\mathrm{Re}[\cdot]$ stands for real part of a complex number. Because $J_1(\boldsymbol{g})$ is a quadratic function of $\boldsymbol{g}$, the optimal solution is given by

$$\boldsymbol{g}_{\text{opt}} = \boldsymbol{Q}^{-1}\boldsymbol{q} \tag{34}$$

So far, the WLS design based on interlaced sampling scheme has been described. In the following, let us study one design example.

3.2 Design Example

Now, a numerical example is used to compare the proposed WLS design with conventional WLS design based on Shannon sampling scheme. The filter coefficients of the conventional WLS are obtained by minimizing the following cost function:

$$J_2(\boldsymbol{h}) = \int_{-\pi}^{\pi} W(\omega)\,|\,H(e^{j\omega}) - H_d(\omega)\,|^2\ d\omega \tag{35}$$

where frequency response $H(e^{j\omega})$ is given in Eq.(2) and vector $\boldsymbol{h} = [h(0) \quad h(1) \quad \cdots \quad h(N)]^T$. Because this is the standard least squares FIR filter design problem, its optimal solution can be obtained easily by using the method in the textbook [11]. Moreover, the integrals in Eq.(33) and Eq.(35) are computed by using numerical rectangular integration method with step size $\frac{\pi}{1000}$. Let us study an example below:

Example 2: In this example, the filter parameters are chosen as $N_{1b} = 10$, $N_{1u} = 20$, $N_{2b} = 13$, $N_{2u} = 17$, $\tau = 0.5$, $N = 30$ and uniform weighting function is used, i.e., $W(\omega) = 1$. Fig.5(a) shows the NRMS error curve E of the proposed WLS method for various delay D. Fig.5(b) is the NRMS error of conventional WLS method based on Shannon sampling scheme. It is clear that the error of proposed WLS method is smaller than the conventional WLS method. Fig.6(a)(b) show the magnitude response and group delay of fractional delay filter designed by proposed method for $N_{1b} = 10$, $N_{1u} = 20$, $N_{2b} = 13$, $N_{2u} = 17$, $\tau = 0.5$, and $D = 15.3$. Fig.6(c)(d) show the magnitude response and group delay of fractional delay filter designed by conventional WLS method for $N = 30$ and $D = 15.3$. Obviously, the proposed method has smaller design error in the high frequency range than Shannon sampling method. That is, wideband design can be accomplished by proposed WLS method based on interlaced sampling scheme. Now, the complexity comparison is presented. Because $N_{1b} = 10$, $N_{1u} = 20$, $N_{2b} = 13$, $N_{2u} = 17$ and $N = 30$ are chosen, the number of adders and multipliers to implement the filters $G_1(z)$ and $G_2(z)$ are 14 and 16, while the number of adders and multipliers to implement filter $H(z)$ are 30 and 31. It is clear that the implementation complexity of $G_1(z)$ and $G_2(z)$ is smaller than that of $H(z)$. Although the accuracy and complexity of proposed WLS method is better than conventional WLS method in the filter part, the proposed method needs one more ADC than the conventional method in the ADC part, as depicted in Fig.1 and Fig.2.

4. CONCLUSIONS

In this paper, the design of wideband fractional delay filter has been investigated. First, the reconstruction formula of interlaced sampling method is applied to design wideband fractional delay filter by using window method. The filter coefficients are easily computed because closed-form design is obtained. Then, the weighted least squares method is used to design wideband fractional delay filters. Finally, numerical examples are demonstrated to show that the proposed method has smaller design error than the conventional fractional delay filter without using interlaced sampling scheme. However, only one-dimensional fractional delay filter is studied in this paper. Thus, it is interesting to extend the proposed method to design two-dimensional fractional delay filters in the future.

REFERENCES

[1] T.I. Laakso, V. Valimaki, M. Karjalainen and U.K. Laine, "Splitting the unit delay: tool for fractional delay filter design," *IEEE Signal Processing Magazine*, pp.30-60, Jan. 1996.

[2] G.D. Cain, N.P. Murphy and A. Tarczynski, "Evaluation of several variable FIR fractional-sample delay filters," *Proc. 1997 IEEE Int. Conf. Acoustic, Speech, and Signal Processing,* pp.III621-624, Apr. 1997.

[3] S.C. Pei, P.H. Wang and H.S. Lin, “Closed-form design of maximally flat FIR fractional delay filter,” *IEEE Signal Processing Letters*, vol.13, pp.405-408, July 2006.

[4] T.B. Deng, "Coefficient-symmetries for implementing arbitrary-order Lagrange-type variable fractional-delay digital filters," *IEEE Trans. on Signal Processing*, vol.55, pp.4078-4090, Aug. 2007.

[5] T.B. Deng, "Symmetric structures for odd-order maximally flat and weighted-least-squares variable fractional-delay filters," *IEEE Trans. on Circuits and Systems-I: Regular Papers,* vol.54, pp.2718-2732, Dec. 2007.

[6] C.C. Tseng and S.L. Lee, "Design of fractional delay FIR filter using discrete Fourier transform interpolation method," *Proc. 2008 IEEE Int. Symp. Circuits Syst.,* pp.1156-1159, May 2008.

[7] J.J Shyu, S.C. Pei, C.H. Chan and Y.D. Huang, “Minimax design of variable fractional-delay FIR digital filters by iterative weighted least-squares approach,” *IEEE Signal Processing Letters*, vol.15, pp.693-696, 2008.

[8] Y.D. Huang, S.C. Pei and J.J. Shyu, “WLS design of variable fractional-delay FIR filters using coefficient relationship,” *IEEE Trans. on Circuits and Systems-II: Express Briefs,* vol.56, pp.220-224, Mar. 2009.

[9] R.N. Bracewell, *The Fourier Transform and Its Applications*, Third Edition, McGraw-Hill, 2000.

[10] F. Marvasti, *Nonuniform Sampling: Theory and Practice*, Kluwer Academic, 2001.

[11] P.S.R. Diniz, E.A.B. da Silva and S.L. Netto, *Digital Signal Processing: System Analysis and Design*, Cambridge University Press, 2002.

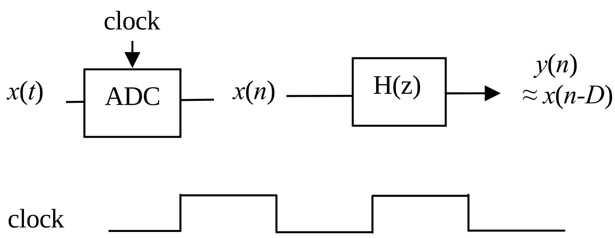

Fig.1 The design of fractional delay filter based on Shannon sampling scheme implemented by one analog-to-digital converter (ADC).

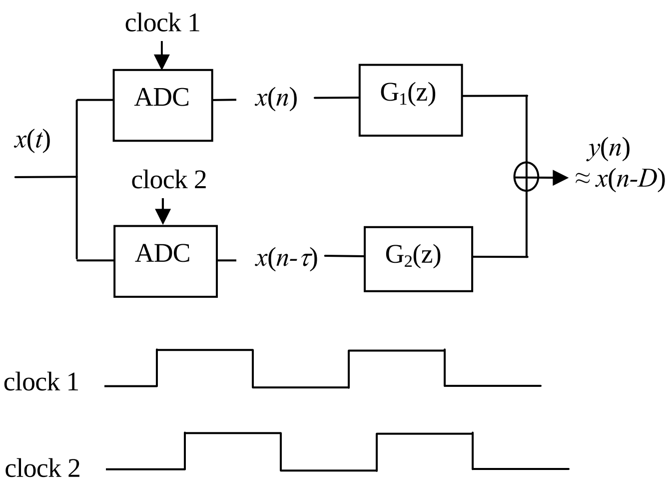

Fig.2 The design of fractional delay filter based on interlaced sampling scheme implemented by two parallel analog-to-digital converters with different control clocks.

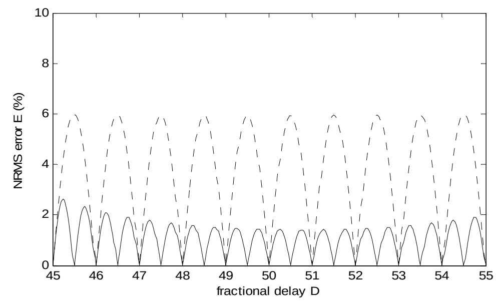

Fig.3 The NRMS error curve E (solid line) of the proposed window method for various delay D . The dashed line is the result of conventional Shannon sampling window method.

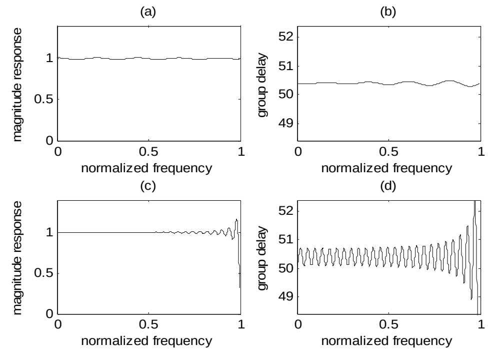

Fig.4 The magnitude response and group delay of the designed fractional delay filters. (a)(b) Proposed interlaced sampling window method. (c)(d) Conventional Shannon sampling window method.

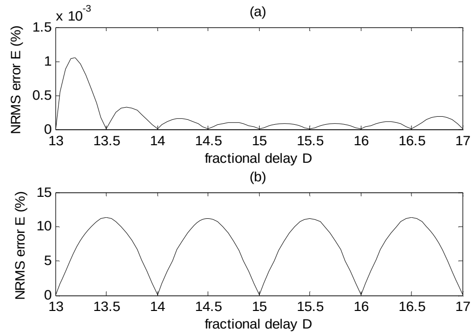

Fig.5 (a) The NRMS error E of the proposed WLS method for various delay D . (b) The NRMS error E of the conventional WLS method for various delay D

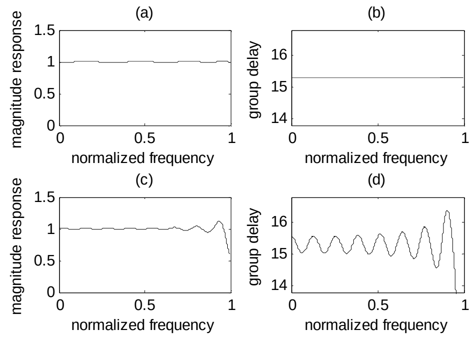

Fig.6 The magnitude response and group delay of the designed fractional delay filters. (a)(b) Proposed WLS method. (c)(d) Conventional WLS method.